NIH-PA Author Manuscript

Carbon nanofiber multiplexed array and Wireless Instantaneous Neurotransmitter Concentration Sensor for simultaneous detection of dissolved oxygen and dopamine

Michael P. Marsh,
Department of Neurosurgery, Mayo Clinic, Rochester, MN 55905

Jessica E. Koehne,
Center for Nanotechnology, NASA Ames Research Center, Moffett Field, CA 94035

Russell J. Andrews,
Center for Nanotechnology, NASA Ames Research Center, Moffett Field, CA 94035

M. Meyyappan,
Center for Nanotechnology, NASA Ames Research Center, Moffett Field, CA 94035

Kevin E. Bennet, and
Department of Neurosurgery, Mayo Clinic, Rochester, MN 55905

Division of Engineering, Mayo Clinic, Rochester, MN 55905

Kendall H. Lee
Department of Neurosurgery, Mayo Clinic, Rochester, MN 55905

Department of Physiology and Biomedical Engineering, Mayo Clinic, Rochester, MN 55905

Abstract

Purpose—While the mechanism of Deep Brain Stimulation (DBS) remains poorly understood, previous studies have shown that it evokes release of neurochemicals and induces activation of functional magnetic resonance imaging (fMRI) blood oxygen level-dependent signal in distinct areas of the brain. Therefore, the main purpose of this paper is to demonstrate the capabilities of the Wireless Instantaneous Neurotransmitter Concentration Sensor system (WINCS) in conjunction with a carbon nanofiber (CNF) multiplexed array electrode as a powerful tool for elucidating the mechanism of DBS through the simultaneous detection of multiple bioactive-molecules.

Methods—Patterned CNF nanoelectrode arrays were prepared on a 4-inch silicon wafer where each device consists of 3×3 electrode pads, 200 μm square, that contain CNFs spaced at 1μm intervals. The multiplexed carbon nanofiber CNF electrodes were integrated with WINCS to detect mixtures of dopamine (DA) and oxygen (O_2) using fast scan cyclic voltammetry (FSCV) *in vitro*.

Results—First, simultaneous detection of O_2 at two spatially different locations, 200 um apart, was demonstrated. Second, simultaneous detection of both O_2 and DA at two spatially different locations, using two different decoupled waveforms was demonstrated. Third, controlled studies demonstrated that the waveform must be interleaved to avoid electrode crosstalk artifacts in the acquired data.

Tel: (507) 293-0512/Fax: (507) 284-9778 lee.kendall@mayo.edu.

Conclusions—Multiplexed CNF nanoelectrode arrays for electrochemical detection of neurotransmitters show promise for the detection of multiple analytes with the application of time independent decoupled waveforms. Electrochemistry on CNF electrodes may be helpful in elucidating the mechanism of DBS, and may also provide the precision and sensitivity required for future applications in feedback modulated DBS neural control systems.

Keywords

Fast Scan Cyclic-Voltammetry; carbon nanofibers; electrochemistry; DBS; multiplexed array electrode

INTRODUCTION

Traditional fast-scan cyclic voltammetry (FSCV) methods have employed a single carbon fiber pulled in a glass capillary for detection of neurotransmitters. While this technique has proven successful for over 20 years, it has many drawbacks. The carbon fiber microelectrode (CFM) can only record from a single location in the brain, and is fragile, making handling and potential human implantation a near impossibility. In recent years, nanoelectrodes using various nanomaterials such as carbon nanotubes, graphene and other inorganic nanowires have been explored to detect neurotransmitters [1]. Among these efforts, a nanoelectrode array (NEA) using vertically aligned carbon nanofibers (CNF) as sensing elements has reached some level of maturity in terms of wafer-scale fabrication and application demonstration [2-7]. The CNFs have previously demonstrated high sensitivity, high spatial resolution, and good biocompatibility [6, 8, 9]. These features have been partially attributed to their bamboo-like structure, in which the open ends of the CNFs have very fast electron transfer rate similar to graphite edge planes [9]. In addition, the CNF electrode is mechanically strong in comparison to the pulled borosilicate glass capillary which can have a wall thickness of less than one micron toward the tip. In its current form, the 3x3 CNF electrode is not suitable for implantation due to its shape and overall size; therefore the experiments in this study were performed *in vitro*. However, the methods to manufacture these electrodes evolve from semiconductor processing techniques, which enables a variety of electrode shapes, sizes, and multiplex options to be batch fabricated at low cost, and thus an electrode useful for *in vivo* applications is not far from reach. Currently, we are developing the next generation penetrating multiplexed carbon nanofiber electrode array that may be deployed using the Leksell stereotactic frame during DBS neurosurgery. Aside from the manufacturing possibilities and mechanical robustness, carbon nanofiber electrodes offer highly advantageous multiplexing capabilities. Multiplexing of arrays of sensing electrodes supports increased spatial resolution for electrochemical recordings. In addition to improvements in spatial resolution, multiplexing can support the application of multiple waveforms.

Deep brain stimulation (DBS) is a state-of-the-art neurosurgical treatment for patients with movement and psychiatric disorders. While the mechanism remains poorly understood, previous studies have shown that DBS evokes release of neurochemicals and induces activation of fMRI blood oxygen level-dependent (BOLD) signal in distinct areas of the brain, including the dopamine rich basal ganglia network [10]. Highly selective electrochemical detection of oxygen and neurotransmitters is now possible with the use of multiplexed arrays. Neural activity has been associated with changes in cerebral blood flow, and electrochemical detection of oxygen is a good indicator of increased blood flow [11]. Here, we present the integration of the Mayo Clinic developed WINCS system and the NASA developed carbon nanofiber 3x3 array for the evaluation of multiplexing capabilities and simultaneous electrochemical detection of DA and O_2 .

Methods

Electrode fabrication

Sensor devices of patterned CNF nanoelectrode arrays were prepared on a 4-inch silicon wafer. Each device consists of 3×3 electrode pads, each 200 μm square, that contain CNFs spaced at 1-μm intervals as shown in Fig. 1a. Detailed fabrication protocols have been described previously [12]. Vertically aligned CNFs were grown from 100-nm diameter, electron-beam defined nickel catalyst areas in a DC-biased plasma-enhanced chemical vapor deposition (PECVD) reactor (BlackMagic Nanoinstruments, Cambridge UK) using ethylene feedstock (125 sccm) and ammonia etchant (444 sccm) at 700 °C, 4.7 Torr and 180 W. CNF length typically ranged from 2.5 to 3.5 μm. The CNFs were encapsulated with dual-RF PECVD-deposited silicon dioxide using O_2 (6000 sccm) and tetraethylorthosilicate (2-3 mL/min) at 400° C, 3 Torr and 1000 W. The oxide was polished using 0.5-μm alumina slurry to expose the tips of the CNFs. Finally, the silicon dioxide covering the contact pads was removed using a dilute 7:1 water:hydrofluoric acid solution (Sigma Aldrich, Saint Louis, MO). The Ag/AgCl reference electrodes, a 31-AWG Teflon-insulated Ag wire (World Precision Instruments, Sarasota, FL, USA), were prepared by chlorination in bleach solution over night.

Microscopy characterization of electrodes

A Hitachi S-4800 field emission scanning electron microscope (SEM) (Hitachi, Pleasanton, CA), operated with 10-kV accelerating voltage and 10-μA beam current, was utilized to visualize the CNF array and CFM. The CFM length and diameter were measured from SEM images using ImageJ software (NIH, version 1.36b), via the freehand selection tool. A Nanoscope atomic force microscope (AFM) (Digital Instruments, Santa Barbara, CA) was used to visualize the protruding CNFs. Images were acquired using a multiwalled carbon nanotube AFM probe (CCHAR, Carbon Design Innovations, Burlingame, CA) in tapping mode by dampening the amplitude 30%. AFM height and amplitude images were collected at a 0.8-Hz scan rate and 512×512 pixels/frame. CNF height was measured using Gwyddion (SourceForge.net) software, using the freehand profile extraction function.

WINCS

WINCS integrates FSCV and digital telemetry to display electrochemical measurements on a base station computer in nearly real time. WINCS hardware incorporates front-end analog circuitry for FSCV, a Bluetooth transceiver and a microcontroller on a small (3.3 cm by 6.5 cm) multilayer printed circuit board (PCB), as shown in Fig. 1b. The PCB and a rechargeable lithium-ion battery are sealed in a polycarbonate case that can be sterilized by the Sterrad® gas plasma process.

A digital-to-analog converter in the microcontroller impresses the FSCV waveform upon the electrochemical sensor, while a transimpedance amplifier converts the resulting current to a voltage signal that is digitized by the microcontroller at a rate of up to 100,000 samples*second^{-1}. The data stream is transmitted to the base station via a Bluetooth® radio link. Custom software, "WincsWare," controls the operational parameters for FSCV, records the transmitted data stream, and displays the data near real time in various formats, including a background-subtracted three-dimensional color plot of sequential FSCV scans. WincsWare can replay stored data files, which may also be ported to applications such as MATLAB®.

Dopamine and Oxygen detection

All electrochemical measurements were made with the WINCS systems. An in-house custom-designed flow cell chamber (Fig. 1c) and a FIAlab 3200 injection system (FIAlab

Instruments, Seattle, WA), with an 8 port switching valve, were used to introduce electroactive molecules to the electrode surface. Dopamine (Sigma Aldrich, Saint Louis, MO), in concentrations ranging from 1 to 5 µM, and O_2 in concentrations ranging from 10-50 µM were prepared in 150-mM sodium chloride (Sigma Aldrich, Saint Louis, MO) and 12-mM Tris (Sigma Aldrich, Saint Louis, MO); the flow cell was purged with this buffer solution for at least 30 seconds prior to each analyte injection. The flow was operated at a rate of 2.25 mL/min using gravity feed for all FSCV experiments. The 8 port switching valve equipped FIAlab 3200 allowed for symmetrical flow paths in both on and off positions as to not interrupt a constant flow rate between injections caused by changes in tubing resistance. Oxygen solutions were produced with an aerated solution of known O_2 concentration continuously monitored with a dissolved O_2 meter (Oakton Instruments, Vernon Hills, IL), and an automated technique to dilute the oxygenated solution with normal buffer at any ratio desired using a two syringe system and custom programming of the FIAlab-3200. The flow cell was assembled with glass syringes and polyether ether ketone (PEEK) tubing (IDEX Health & Sciences, Oak Harbor, Washington) to minimize any loss of O_2 prior to electrochemical detection. The waveforms for DA and O_2 (as shown in Fig. 1d) were applied in a two-electrode configuration against a single Ag/AgCl reference using two WINCS systems running side by side on two base-station computers with Windows OS. An oscilloscope (Tektronix, Beaverton, OR) was used to help visualize the timing of the waveforms with one another for all experiments.

RESULTS AND DISCUSSION

Simultaneous detection of O_2 in two locations

Oxygen in concentrations of 10-50 µM in increments of 10 µM was introduced into the flow cell for electrochemical detection. Simultaneous detection of 30 µM dissolved O_2 at two spatially different locations, 200 µm apart, is shown in Fig. 2a. The two adjacent electrodes shared a common reference, and the waveforms applied were interleaved such that one waveform did not overlap with the other. The responses of the electrodes were nearly identical, suggesting similar electrochemical properties and reproducibility between adjacent sensing elements. The reduction potential of O_2 occurs near the minimum of the N-shape waveform at −1.3V. In the background subtracted cyclic voltammogram (BGS CV; Fig. 2b), a maximum reduction current of −20 nA at a −1.3 V potential can be observed. The current-measured was plateau like for the 10 second injection, with a temporal lag response at the beginning of the injection, slight rise throughout, and ramp down toward the end as seen on the current plot in Fig. 2c. The temporal lag due to the adsorption and desorption of catecholamines on the electrode surface does not reflect that of O_2 [13]. Rather, due to the planar nature of the 3×3 array, and the design of the flow cell chamber to accommodate a flat sensor chip, we expect there to be an increased length of time for equalization of the electrochemical response. This is because the chamber volume of fluid which encapsulates the sensing area of the electrode is approximately 5× larger (measured at 30 µL) than that used in the flow cell for the columnar shaped CFMs. This larger volume slightly increases the time for the individual sensor's microenvironment to equilibrate to the desired concentration that is to be detected during infusion of the analyte. Future flow cell design will try to minimize this chamber volume to yield faster electrode response.

A similar experiment was performed by Zachek et al for the detection of dopamine at spatially different locations. In one case, they developed a microelectrode spacer to align and hold 4 individual electrodes 250 µm apart to record in the rat nucleus accumbens [14]. In the other case, they utilized a silicon based microelectrode array with 4 pyrolyzed carbon as sensing elements for dopamine detection in the rat striatum [15]. In both cases they were able to demonstrate reproducibility and minimal crosstalk between sensing elements as we

were. In addition, they were able to demonstrate the heterogeneity of catecholamine release in both areas of the brain.

With an increased spatial resolution of electrode arrays, and sub-second FSCV temporal response, the matrix of sensing pads may help distinguish the foci of the neurotransmitter release, increase the probability of detecting release, and provide dimension to the propagation of heterogeneous neurotransmitter release events. For example, one very common procedure used in small animal DBS research is the detection of evoked DA release in the rat brain striatum from electrical stimulation in the medial forebrain bundle. The optimized areas of dense dopamine terminals, commonly called the "hot spot", where large amounts of dopamine can be detected, can be difficult to locate. A multiplex array may very easily improve the chances of neurotransmitter detection in these types of experiments. We expect a similar result after our carbon nanofiber array is repackaged as a penetrating electrode and *in vivo* experiments are performed.

Simultaneous detection of O_2 and DA

Simultaneous detection of a mixture of DA and O_2 at concentrations of 3 μM and 10 μM respectively at two spatially different locations, using decoupled waveforms is demonstrated in Fig. 2d. The triangle shape and N-shape waveforms were applied on adjacent electrodes to separately detect DA and O_2, respectively. The BGS CV shown in Fig. 2e, portrays the signature voltammogram of both O_2 and DA. The reduction of oxygen occurs near the −1.3 V switching potential, whereas the oxidation and reduction of DA occur near 0.6V and −0.2V respectively. The major advantage of simultaneously applied decoupled waveforms is the ability to optimize each to detect a specific analyte. The array style electrode could be further pretreated with functional groups for enhanced sensitivity of specific neurotransmitters release/uptake events [16].

A calibration curve for the detection of DA is shown in Fig. 3a and O_2 in Fig. 3b, normalized with respect to the surface area calculated with SEM and AFM techniques. The correlation coefficients for both were better than 0.98, indicating high linear response of the current to the increase in concentration of the analyte. To test whether there is interference between the two contacts as they measure different analytes, we varied the concentration of one analyte while holding the other constant. Figure 3c demonstrates the detection of increasing concentrations of O_2 from 10-50 μM in increments of 10 μM in the presence of 3 μM DA. The detected current remained linear for both DA and O_2, suggesting good predictable detection response in variable mixtures.

Similar experiments for the simultaneous detection of DA and O_2 have been performed. In 1991, Zimmerman and Wightman were able to detect oxygen and dopamine transients in the rat striatum with a single electrode [17]. They applied a single triangular waveform that sweeps from +0.8 V to −1.4 V with a 0.0 V resting potential which enables the detection of both oxygen and dopamine in a single voltammogram. In our case, we applied two separate waveforms on two adjacent electrodes, which enable the use of optimized waveforms for improved sensitivity. Many waveforms have been established for the detection of specific analytes of interest such as adenosine [18], oxygen [11], and serotonin [19]. For instance, a standard waveform for detection of DA is the triangle shape, with a 300 V/s ramp rate, a −0.4V holding potential, with a 1.0V peak as used here. With the ability to apply different waveforms on adjacent electrodes, one can increase the selectivity and sensitivity for multiple analytes during a single neurobiological event, such as evoked neurotransmitter release during DBS.

In another similar experiment performed by Zachek et al, two different waveforms were applied for the detection of oxygen and dopamine on adjacent electrodes using a micro

fabricated electrode array with pyrolyzed carbon sensing elements *in vitro* [20]. Data acquisition was carried out with a hardwired biopotentiostat and Quad UEI head stage amplifier, and the applied waveforms were not the same as used in our experiment, each having a −0.4 V resting potential with different peak voltages and ramp rates. Both of our results were nearly identical, successfully demonstrating the use of multiple waveforms on adjacent electrodes in the same electrochemical cell with reproducibility and minimal crosstalk.

Crosstalk Evaluation with Interleaved FSCV

The possibility of crosstalk was evaluated during electrochemical detection of DA and O_2 with two waveform timing configurations. Figure 4a and 4b show the triangle-shape and N-shape waveform arrangement when they were either interleaved or overlapped respectively, as visualized with the aid of an oscilloscope. It can be seen in Fig. 4c that when the waveforms are interleaved, the pseudo-color plots are unaffected, and no additional artifacts are seen. Whereas, when the waveforms overlap one another, an artifact obscures the view of data as observed in Fig. 4d. Although the electrodes are separated by some distance, they are not electrically isolated. The artifacts occur not at a particular set voltage, but at a specific time, when the waveform slope potential changes direction. The N-shape waveform potential changes directions 4 times during a single scan, where as the Triangle-shaped waveform changes only 3 times. In Fig. 4d, one can observe 4 artifacts in the triangle-shape color plot; these occur during the 4 voltage direction changes during the simultaneous application of the N-shape waveform. In the bottom right color plot of Fig. 4d, one can observe 2 horizontal artifacts; these occur during 2 of the 3 voltage direction changes during the simultaneous application of the Triangle-shape waveform. The third voltage change artifact is not seen because the time span for a complete triangle-shape waveform is longer than that of a complete N-shape waveform, thus it is not detected. Ultimately, for the application of two different waveforms, it is important that they are applied in a staggered manner such that they do not over lap. Conversely, in order to apply two waveforms at the exact same time without the observation of an artifact, the waveforms must start and end together, and share the exact same shape. The application of waveforms in this manner has been shown possible with other bio-potentiostat systems, such as the EI-400 (ESA, Chelmford, MA) and Quad UEI head stage amplifier supplied by the University of North Carolina Department of Chemistry [20].

For the application of multiple different waveforms, we are confined to the amount of time between scans. Commonly, FSCV waveforms are applied 10 times per second, and require approximately 10ms per scan. In this case, it would limit a system to ten different waveform applications on a single multiplexed electrode. This is adequate for most current demands in electrochemistry, and for an instance where large multiplex arrays with more than 10 sensing elements are needed, one may still apply the exact same waveform across each as long as they are synchronous. Additional experiment, not shown, has demonstrated that the artifact generated can be eliminated with the use of two separate reference electrodes. Future electrode designs which employ multiple sensor areas may benefit if each has its own separate reference electrode. This would increase the options for applying multiple waveforms simultaneously with without the need for interleaving scans.

CONCLUSION

Carbon nanofiber electrode arrays show promise for the electrochemical detection of multiple neurotransmitters through application of time independent decoupled waveforms, improving detection sensitivity and selectivity by utilizing optimized waveforms for each particular analyte of interest. Results here have demonstrated that different waveforms can

be applied simultaneously using WINCS to adjacent electrode pads with minimal crosstalk for the detection of mixtures of DA and O_2. In conjunction with the ability to apply different waveforms for detection of multiple neurotransmitters, the CNF array has the capability of providing increased spatial resolution for neurochemical detection, and may help to improve our understanding of both the pathophysiology of disorders of the nervous system and further elucidate the mechanism of DBS. Future integration of DBS and multiplexed FSCV electrodes may lay the foundation for the development of an implantable "smart" DBS system that utilizes neurochemical feedback control.

Acknowledgments

REFERENCES

1. Zhang H. Carbon nanofibers based micro/nanodevices for neural electrical and neural chemical interfaces. Journal of Nanomaterials. 2012; 2012:1–6.

2. Koehne J, et al. Ultrasensitive label-free DNA analysis using an electronic chip based on carbon nanotube nanoelectrode arrays. Nanotechnology. 2003; 14(12):1239–45. [PubMed: 21444977]

3. Koehne JE, et al. The fabrication and electrochemical characterization of carbon nanotube nanoelectrode arrays. Journal of Materials Chemistry. 2004; 14:676–684.

4. Koehne JE, et al. Carbon nanofiber electrode array for electrochemical detection of dopamine using fast scan cyclic voltammetry. Analyst. 2011; 136(9):1802–5. [PubMed: 21387028]

5. Nguyen-Vu TD, et al. Vertically aligned carbon nanofiber arrays: an advance toward electrical-neural interfaces. Small. 2006; 2(1):89–94. [PubMed: 17193561]

6. Nguyen-Vu TD, et al. Vertically aligned carbon nanofiber architecture as a multifunctional 3-D neural electrical interface. IEEE Trans Biomed Eng. 2007; 54(6 Pt 1):1121–8. [PubMed: 17554831]

7. Siddiqui S, et al. Characterization of carbon nanofiber electrode arrays using electrochemical impedance spectroscopy: effect of scaling down electrode size. ACS Nano. 2010; 4(2):955–61. [PubMed: 20099879]

8. Koehne JE, et al. Miniaturized multiplex label-free electronic chip for rapid nucleic acid analysis based on carbon nanotube nanoelectrode arrays. Clin Chem. 2004; 50(10):1886–93. [PubMed: 15319319]

9. Li J, et al. Inlaid multi-walled carbon nanotube nanoelectrode arrays for electroanalysis. Electroanalysis. 2005; 17(1):15–27.

10. Lee KH, et al. Emerging techniques for elucidating mechanism of action of deep brain stimulation. Conf Proc IEEE Eng Med Biol Soc. 2011; 2011:677–80. [PubMed: 22254400]

11. Venton BJ, et al. Real-time decoding of dopamine concentration changes in the caudate-putamen during tonic and phasic firing. J Neurochem. 2003; 87(5):1284–95. [PubMed: 14622108]

12. Arumugam PU, et al. Wafer-scale fabrication of patterned carbon nanofiber nanoelectrode arrays: a route for development of multiplexed, ultrasensitive disposable biosensors. Biosens Bioelectron. 2009; 24(9):2818–24. [PubMed: 19303281]

13. Venton BJ, Troyer KP, Wightman RM. Response times of carbon fiber microelectrodes to dynamic changes in catecholamine concentration. Anal Chem. 2002; 74(3):539–46. [PubMed: 11838672]

14. Zachek MK, et al. Simultaneous monitoring of dopamine concentration at spatially different brain locations in vivo. Biosens Bioelectron. 2010; 25(5):1179–85. [PubMed: 19896822]

15. Zachek MK, et al. Microfabricated FSCV-compatible microelectrode array for real-time monitoring of heterogeneous dopamine release. Analyst. 2010; 135(7):1556–63. [PubMed: 20464031]

16. Roberts JG, et al. Specific oxygen-containing functional groups on the carbon surface underlie an enhanced sensitivity to dopamine at electrochemically pretreated carbon fiber microelectrodes. Langmuir. 2010; 26(11):9116–22. [PubMed: 20166750]

17. Zimmerman JB, Wightman RM. Simultaneous electrochemical measurements of oxygen and dopamine in vivo. Anal Chem. 1991; 63(1):24–8. [PubMed: 1810167]

18. Swamy BE, Venton BJ. Subsecond detection of physiological adenosine concentrations using fast-scan cyclic voltammetry. Anal Chem. 2007; 79(2):744–50. [PubMed: 17222045]

19. Hashemi P, et al. Voltammetric detection of 5-hydroxytryptamine release in the rat brain. Anal Chem. 2009; 81(22):9462–71. [PubMed: 19827792]

20. Zachek MK, et al. Simultaneous decoupled detection of dopamine and oxygen using pyrolyzed carbon microarrays and fast-scan cyclic voltammetry. Anal Chem. 2009; 81(15):6258–65. [PubMed: 19552423]
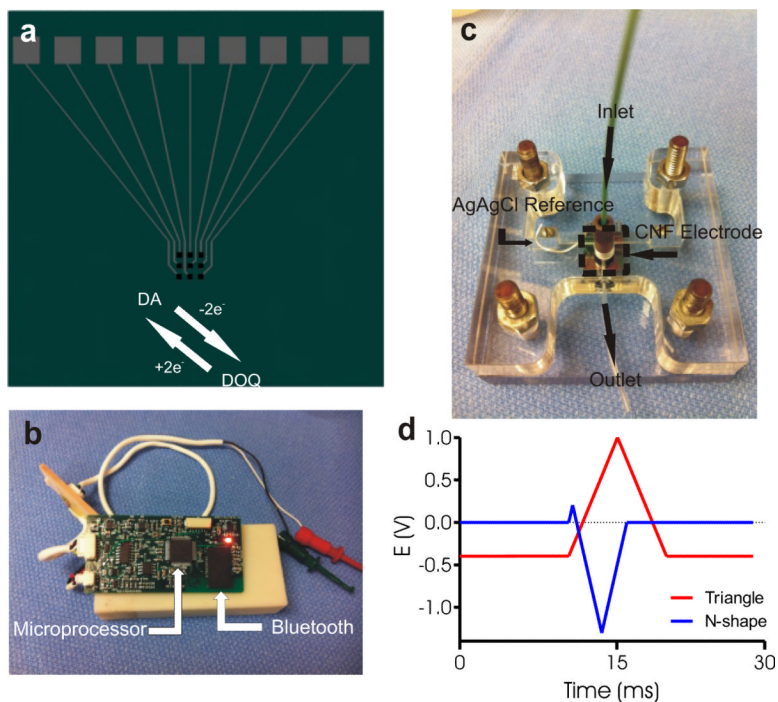
Fig 1.
WINCS device for detection of dopamine and oxygen. (a) Schematic of carbon nanofiber electrode and dopamine redox reaction. (b) Printed circuit board indicating the FSCV microcontroller and the Bluetooth module for wireless communication with a data-acquisition computer. (c) Image of the custom made flow cell chamber housing the 3x3 microelectrode array (d) Applied voltage waveform for dopamine and oxygen detection. The FSCV waveform for dopamine detection is a pyramidal excursion ("scan") from a baseline potential of −0.4 V to a peak of +1.0 V and back to baseline, at a "scan rate" of 300 V/s. The waveform used for oxygen is an N-shape excursion with a 0.0 V holding potential, first scanned to +0.2 V, then down to −1.3 V, and back to 0.0 V, at a "scan rate" of 450 V/s. Scans were repeated 10 times per second.
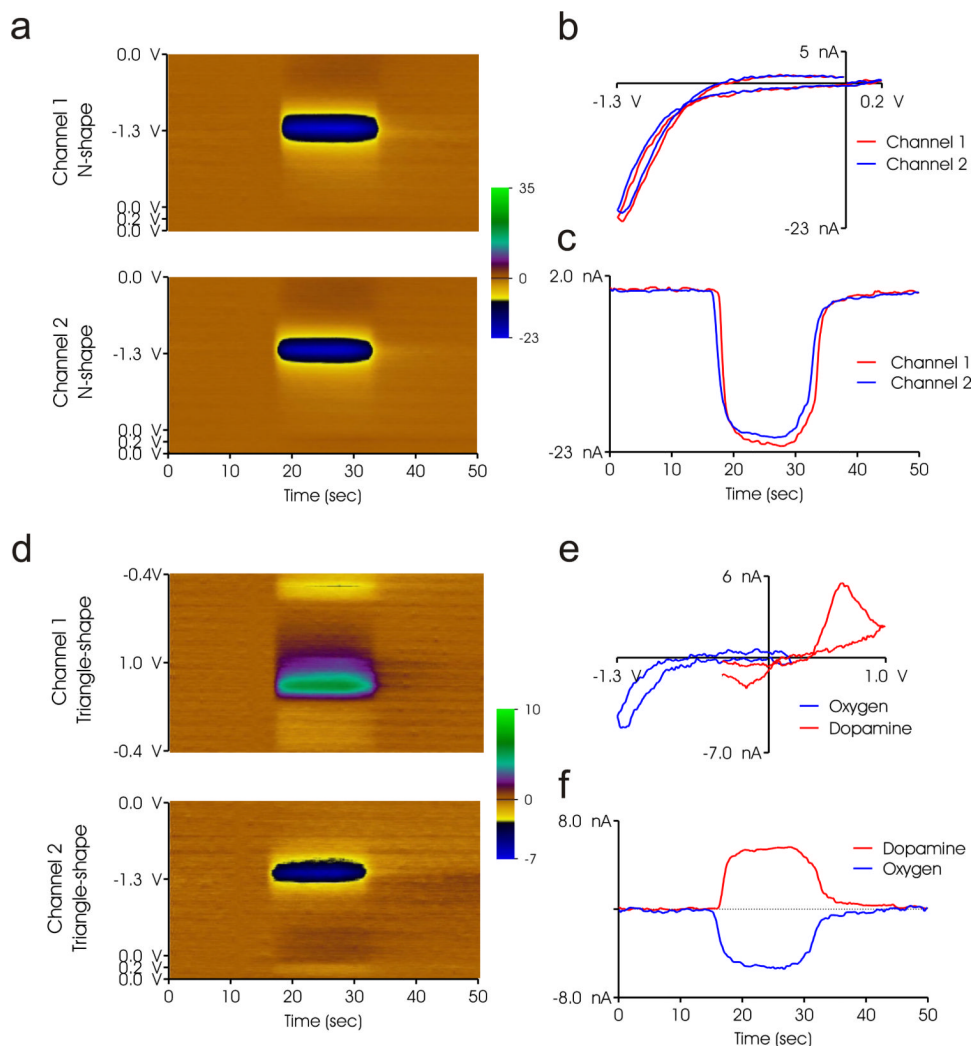
Fig 2.
(a) Pseudo color plots of simultaneous detection of dissolved oxygen on two adjacent CNF electrodes with applied N-shape waveform, channels 1 and 2. (b) Background subtracted voltammograms of O_2 detected on channels 1 and 2. (c) Strip chart current plots of O_2 detection on channels 1 and 2. (d) Simultaneous detection of dissolved DA and O_2 on two adjacent CNF electrodes with triangle-shape and N-shape waveforms applied respectively on channels 1 and 2. (e) Background subtracted voltammograms of DA and O_2 detected on channels 1 and 2. (f) Strip chart current plots of DA and O_2 detection on channels 1 and 2.
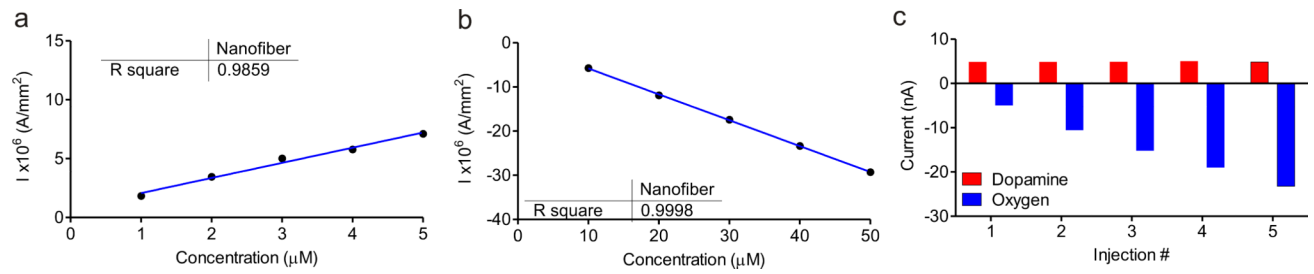
Fig 3.
(a) DA calibration curve for the CNF array from 1 to 5 μM in increments of 1 μM, normalized with respect to surface area. (b) O_2 calibration curve for the CNF array with concentrations from 10-50 μM in increments of 10 μM, normalized with respect to surface area. (c) Plot demonstrating the detection of increasing concentrations of O_2 (10-50 μM) while holding DA concentration constant at 3 μM.
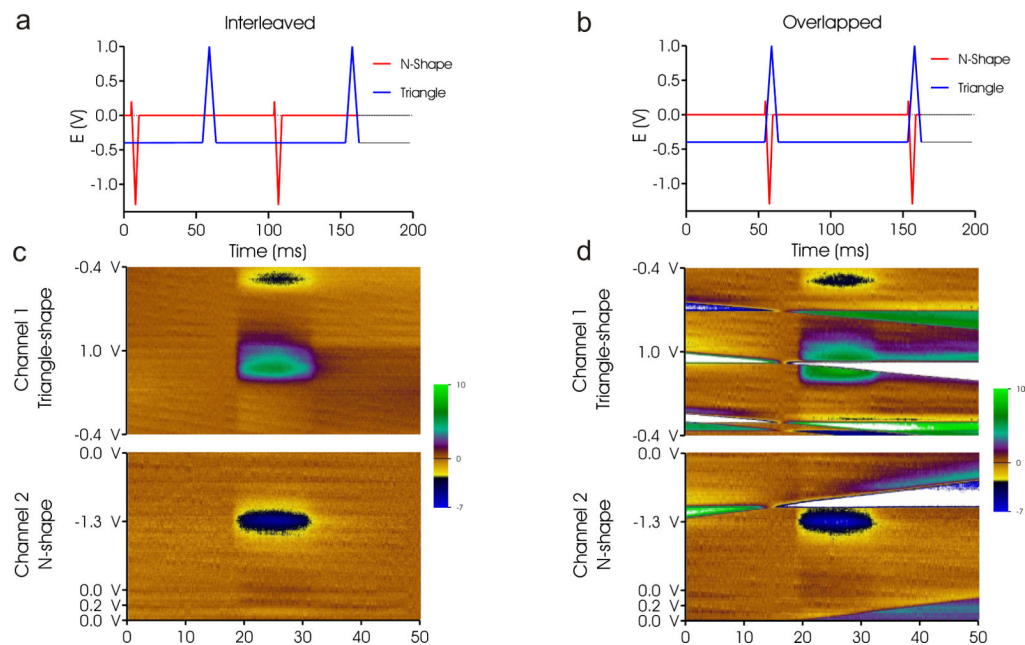
Fig 4.
Crosstalk evaluated at the CNF electrodes. (a) The N-shape and Triangle shape waveforms when they are interleaved. (b) The N-shape and triangle-shape waveforms when they are overlapped. (c) Dopamine and oxygen detection when the applied waveforms are interleaved. (d) Dopamine and oxygen detection when the applied waveforms are overlapped.